



# Intelligent Imaging Method of Nuclear Magnetic Resonance Medical Devices Based on Compression Sensing

Xuchu Deng<sup>1</sup>(✉), Zongying Lai<sup>1</sup>, and Lizhi Chen<sup>2</sup>

<sup>1</sup> School of Ocean Information Engineering, Jimei University, Xiamen 361012, China  
dd612p@163.com

<sup>2</sup> Chengdu Neusoft University, Chengdu 611844, China

**Abstract.** Aiming at the problems of low peak signal-to-noise ratio and slow imaging speed in the imaging method of nuclear magnetic resonance medical devices, an intelligent imaging method of nuclear magnetic resonance medical devices based on compression sensing is designed. The imaging space of nuclear magnetic resonance medical devices is limited to two dimensions, and the nuclear magnetic resonance pulse sequence is designed to determine the current proton state by receiving the energy attenuation signal. The imaging data is compressed and sampled, and the original signal is reconstructed according to the collected data and the measurement matrix to ensure the image quality. Finally, the intelligent imaging mode based on compressed sensing optimization is realized. The experimental results show that the peak signal-to-noise ratio of the intelligent imaging method of NMR medical devices in this paper is higher than that of the other two intelligent imaging methods of NMR medical devices, which proves that the performance of the intelligent imaging method of NMR medical devices can be improved after combining the compression sensing technology.

**Keywords:** Compression sensing · Nuclear magnetic resonance · medical apparatus and instruments · Intelligent imaging · Gradient magnetic field · Natural signal

## 1 Introduction

The intelligent imaging method of nuclear magnetic resonance medical devices based on compression sensing can present various dynamic processes, including the physiological movements of tissues and organs (such as heart, bone and joint, swallowing, etc.), as well as the changes of contrast agents and surgical intervention, which has broad application prospects. Compression sensing collects and compresses signals during signal acquisition, combining sampling and compression, greatly reducing the number of samples and data storage. However, the problem of long imaging time has been restricting the further development of MRI. On the one hand, the long imaging time greatly increases

the possibility of patient movement during the imaging process, causing artifacts, blurring and other problems in the image, and even having to sacrifice image quality to shorten the imaging time, but it causes the lack of diagnostic information. Applying compressed sensing to image and video fields can effectively reduce data acquisition costs and data storage costs. Compression sensing can sample data at a frequency much lower than Nyquist's, and is widely used in image compression, medical imaging, atomic force microscope imaging, radar imaging, pattern recognition, channel coding and many other fields. It is considered to be an important key technology to promote the development of social informatization. On the other hand, the long imaging time limits the time resolution of imaging, resulting in the inability to fully present the real dynamic process, which directly hinders the trend of real-time dynamic imaging to clinical application [1, 2]. Therefore, accelerating the speed of magnetic resonance imaging has important theoretical significance and practical value for improving image quality, improving time resolution, and expanding the application field of magnetic resonance medical device imaging.

The imaging time of magnetic resonance medical devices is mainly composed of scanning time and image reconstruction time. In the theory of compressed sensing, the measured signal is required to be sparse or compressible. In practice, most signals are not strictly sparse, but studies have shown that most natural signals are compressible. That is, although it is a non sparse signal in the time domain, the signal can be sparse after a series of domain transformations, such as discrete cosine transform, discrete wavelet transform and curvelet discrete transform. In principle, dynamic imaging is the repeated application of conventional static imaging methods, that is, a frame of data is completely scanned, and then the image is directly reconstructed by inverse Fourier transform. Due to the application of fast Fourier transform, the imaging time mainly depends on the scanning time. That is to say, most natural signals are sparse in Fourier domain, discrete cosine domain, discrete wavelet domain and curvelet basis. Another representation of signal sparsity, redundant dictionary representation, is also a commonly used signal sparse transformation method. In order to meet the real-time requirements, the scanning speed is required to be higher than the physiological movement speed. However, hardware (gradient magnetic field intensity and its switching rate) and physiological (such as nerve stimulation) factors limit the application of fast scanning. No matter two-dimensional image or three-dimensional image, as long as the conditions of compressed sensing are met, the measurement of data can be greatly reduced, so as to shorten the reconstruction time. Therefore, how to shorten the scanning time and image reconstruction time and improve the imaging speed has become the main research problem of magnetic resonance medical device imaging. In this paper, an intelligent imaging method of nuclear magnetic resonance medical devices based on compression sensing is proposed. The imaging space of nuclear magnetic resonance medical devices is limited to two dimensions, and the nuclear magnetic resonance pulse sequence is designed to determine the current proton state by receiving the energy attenuation signal. The imaging data is compressed and sampled, and the original signal is reconstructed according to the acquired data and measurement matrix to ensure the image quality. The results show that the mean value of the peak signal-to-noise ratio of the method studied is high, which proves that the performance of the intelligent imaging method of nuclear magnetic resonance medical

devices is improved after the combination of compression sensing technology. Fast imaging speed and high quality of reconstructed images are of great significance both from the perspective of patients and doctors.

## 2 Collect Magnetic Field Imaging Signal

Imaging with magnetic resonance technology actually reflects the distribution of hydrogen atoms in the body. Usually, at a certain resonance frequency, RF excitation often excites the whole solid, so we can use the gradient transformation to selectively excite a part of the solid when we locate the hydrogen atom in space. If the sampling is dense enough, a continuous signal can be represented by its sampling values at equal time intervals, and all the signals can be recovered through these sample values, which is the content of the sampling theorem. Therefore, in magnetic resonance imaging, three gradient magnetic fields are used for imaging operation. One gradient magnetic field is used to determine the plane. After determining the plane through the gradient magnetic field, the imaging space is limited to two dimensions. Then the corresponding signals are spatially encoded in this two-dimensional plane, and this process realizes the collection of data at a specific level. The importance of sampling theorem is that it acts as a bridge between continuous time signals and discrete-time signals [3–5]. Under certain conditions, a continuous time signal can be completely recovered from its samples, which provides a theoretical basis for discrete signals to represent continuous signals, because in many aspects, the processing of discrete signals is more flexible and convenient than that of continuous signals. The static magnetic field is the external magnetic field, pointing in the longitudinal direction, and its magnetic field strength determines the net magnetic moment and resonance frequency of the atomic nucleus. The uniformity of magnetic field is particularly important for imaging. If the magnetic field is uneven, the imaging image will often produce deformation or artifacts. In the process of magnetic resonance imaging, due to external factors, the external magnetic field strength is often difficult to achieve complete uniformity. According to the multiplication property of Fourier transform, the spectrum calculation formula of finite frequency band is obtained:

$$L(\delta) = \frac{1}{2\pi} \left[ D(\delta) \times \sqrt{G(\delta - 1)^2} \right] \quad (1)$$

In Eq. (1),  $D$  represents continuous time signal,  $G$  represents sampling frequency, and  $\delta$  represents periodic function. The concept of sampling makes people think of using discrete-time system technology to realize continuous time and indirectly process continuous time signals: first, convert continuous time signals into discrete-time signals through sampling, then use discrete-time system to process the discrete-time signals, and finally convert discrete-time signals into continuous time. Therefore, in order to ensure a good MRI effect, the uniformity of the external magnetic field must be guaranteed within a specific range. Gradient magnetic field is generated by several groups of coils located in the magnet cavity through current. Attached to the main magnetic field, it can increase or decrease the strength of the main magnetic field, so that the spin protons along the gradient direction have different magnetic field strengths, so there are different types of resonance frequencies. The structure of human eyes leads people to understand

that images are not as sensitive to uniform or linear changes in the image field as data stored on binary media. For example, it is insensitive to some distortions and cannot detect some subtle changes in the image. Even if these subtle changes are directly lost, the human eye cannot feel them. Through the purposeful change of the static magnetic field, we can change the uniformity of the magnetic field, and then interpret the spatial information of the signal through the transformation law of the static magnetic field strength, so as to obtain the spatial code of the signal. RF coil can also be used as receiving coil (induction coil) under normal circumstances. For one-dimensional signals, the characteristic information is represented by the sensing matrix, and the expression formula of linear measurement sparsity is:

$$Y = \varepsilon \times \frac{H}{2} \quad (2)$$

In Eq. (2),  $\varepsilon$  represents the orthogonal basis composed of column vectors, and  $H$  represents the original signal. Therefore, within a certain range, the image changes caused by quantization errors cannot be detected by human eyes. The usual way of recording raw data is based on the assumption that the human visual system is uniform and linear, which leads to the equal treatment of the visually insensitive part and the visually sensitive part, resulting in more data than the ideal coding. This redundancy is called visual redundancy. According to Ferrari's law of electromagnetic induction, the change of magnetic flux in a closed circuit will produce induced electromotive force. Therefore, place a coil in a suitable position within the range swept by the transverse magnetization component. Make the coil cut the magnetic induction line, and the induced electromotive force will be generated in the coil, so that the magnetic resonance signal can be detected. In the process of free precession, the decrease of transverse magnetization vector makes the electromotive force received by its coil also decrease. This signal is called free induction attenuation signal. In order to reconstruct the original signal, it is necessary to calculate all the projection data, then select several data with large amplitude, and encode their positions, while all the remaining projection data with small amplitude are discarded. Then through the ring coil to collect the free attenuation signal, the changing magnetic field intensity signal will be obtained, and then the magnetic field intensity signal will be converted into the corresponding electrical signal to complete the signal acquisition. The received signal is the superposition of the overall magnetization vector. Therefore, the entire detection system can detect spatial information only when each magnetic field is a gradient magnetic field.

### 3 Extracting NMR Pulse Sequence

Nuclear magnetic resonance refers to the phenomenon of resonance absorption transition between Zeeman levels under certain conditions. RF pulse, coding gradient field, parameter setting during signal acquisition and their sequence are called pulse sequence of nuclear magnetic resonance. In magnetic resonance imaging, in order to observe the current state of protons, RF pulses are usually used as excitation elements. When the frequency of RF pulses is the same as the precession frequency of protons, resonance will occur [6]. The space allowed to receive digitized original data is  $k$  space, and its

unit is spatial frequency (hz/cm). The pulse sequence includes  $90^\circ$  pulse and  $180^\circ$  pulse. After  $90^\circ$  pulse excitation, the elapsed time: apply another  $180^\circ$  RF pulse, the proton will flip  $180^\circ$  in the transverse plane, and then after time, the spin echo signal will be generated. The generation of resonance will transfer the energy of the RF pulse to the proton. After removing the RF pulse, this part of energy will decay slowly. Therefore, by receiving the decay signal of this part of energy, the current proton state can be determined. Assuming that the external magnetic field intensity is  $Z_0$ , the proton precesses at the angular velocity of  $\eta_0$ . Using a magnetic field with a magnetic field strength of  $Z_1$ , an RF pulse is generated, and the pulse angular velocity is  $\eta_1$ . By using the pulse sequence, changing the interval between the two pulses, the peak signal of the spin echo at each time interval is obtained, and the echo signal is obtained by connecting each peak point. Human body imaging needs to determine the spin density, not the size of the magnetization vector. To obtain proton density weighted images, pulse sequences with long repetition time and short echo time should be used. The magnetic field  $Z_1$  is much smaller than the field strength of the external magnetic field. To generate resonance, the frequency of the RF pulse must be the same as the precession frequency, that is, the angular velocity must be the same. When the two frequencies are the same, the proton precession direction will deflect towards the  $Z_1$  magnetic field. That is, when  $\eta_0 = \eta_1$ . Resonance will occur, and the proton precession direction will deflect. Since the external magnetic field is a stable magnetic field, and the magnetic field strength  $Z_1$  is much smaller than the external magnetic field strength  $Z_0$ , the influence of precession reversal on the external magnetic field strength can be ignored. With the increase of the action time of the magnetic field  $Z_1$ , the deviation of the proton precession direction is also increasing, and the magnetization vector in the corresponding action direction is also gradually increasing. Finally, the proton precession direction is overturned into the same plane. According to the RF pulse intensity and action time, the turning angle  $\gamma$  can be determined, and the formula is as follows:

$$\gamma = \frac{\phi \times h \times l}{2} \quad (3)$$

In Eq. (3),  $\phi$  represents the gyromagnetic ratio,  $h$  represents the intensity of RF pulse, and  $l$  represents the action time of RF pulse. In the relaxation process, we call the phenomenon that the vertical component of the magnetization vector gradually increases and returns to the level before excitation as longitudinal relaxation. The phenomenon that the horizontal component of the magnetization vector gradually decreases until it disappears is called transverse relaxation. Nowadays, the pulse sequences that can obtain proton density weighted imaging are mainly spin echo pulse sequence and gradient echo pulse sequence. The basic idea of gradient echo pulse sequence is to form echo through the reverse of frequency coding gradient. When the magnetization vector returns to the original state in the vertical direction, its vector just disappears in the horizontal direction, so the time required for the longitudinal relaxation process is the same as that for the transverse relaxation process [7, 8]. When the RF pulse acts, the corresponding magnetization vector will deflect. The gradient echo sequence of  $90^\circ$  pulse is a simple pulse sequence. RF pulse is a sinc function in time domain, corresponding to square pulse in frequency domain. The phase coding gradient is represented by a series of horizontal lines, indicating that it steps in incremental rules in different repetition periods. Through

the phase coding and frequency coding, the specific spatial coding at the specific level is formed. Spatial frequency is a vector, which refers to the phase change per unit length in a certain direction. When generating NMR images, two gradient fields of frequency and phase are used. The original data are collected in the frequency domain and can be directly stored in  $k$  space. The reconstructed images can be obtained by Fourier transform of these data. The data with positive phase of spatial coding will be filled to the top of the specific space, and the data with negative phase will be filled to the bottom of the specific space. In this particular space, the signal of the middle row is the strongest. In most cases, the main data are concentrated in the center of the specific space. The NMR signals encoded by three gradients carry the information of layer, frequency and phase respectively. The image can be obtained by Fourier transform of the data stored in  $k$  space. Fourier transform can be used between the reconstructed image and its corresponding  $k$  space, which is the remarkable feature of  $k$  space.

#### 4 Recognizing Dynamic Features of Medical Device Images

According to the time relationship between signal acquisition and imaging, the imaging methods of magnetic resonance medical devices can be roughly divided into two categories: offline and online. In the process of horizontal and vertical relaxation, the atomic nucleus releases energy and transitions from the high-energy state to the original equilibrium state. The process of medical image reconstruction is to complete intelligent imaging by analyzing the voltage signal released in this process. Online imaging method is to reconstruct the image separately for the single frame data at the current time, that is, the form of reconstruction while sampling. When the reconstruction speed of online imaging is fast enough to be faster than the data acquisition speed, this method can be called real-time imaging. The NMR signal is jointly contributed by the spin in the excited volume of the sample. The relationship between the signal and the spin density is as follows:

$$W = \int \frac{\phi \times h \times l}{2} - |\vec{\mu}| \times \varpi^3 \quad (4)$$

In Eq. (4),  $\mu$  represents time-frequency domain signal and  $\varpi$  represents time-domain signal. There is no phase shift in spatial coding, and the data obtained after frequency coding will usually be filled into the middle of a specific space. By applying a certain frequency of RF signal, the plane geometric distribution of the whole human body structure can be obtained. However, it is impossible to image the designated part to be detected, so the received signal must be spatially located. Real time magnetic resonance imaging of medical devices has a wide range of applications, such as dynamic imaging of human joint function, quantitative analysis of cardiovascular blood flow, magnetic resonance guided cardiac surgery and so on. At present, the magnetic resonance imaging system in medicine completes the positioning and coding of spatial information by applying three gradient magnetic fields that are perpendicular to each other and change linearly. Generally, for an image signal, the energy is mainly concentrated in the low-frequency band, that is, the central area of  $k$  space. The high-frequency part of the image contains less energy distribution, that is, the surrounding part of  $k$  space. This

paper first reconstructs the frame difference image, and then obtains the current frame image by adding the reconstructed frame difference image to the previous frame image. Therefore, the previous images are the basis of the whole movie reconstruction, and their reconstruction quality will affect the reconstruction quality of the next frame image of the movie. Therefore, the traditional equal interval uniform density scanning sampling method often leads to the generation of image aliasing artifacts. Therefore, this paper considers using a variable density sampling method to collect more low-frequency bands with high information and less high-frequency bands with low information, which may obtain a more accurate reconstruction effect and reduce the generation of image aliasing artifacts. Therefore, this paper constructs an imaging mode in which the sampling rate gradually decreases to a stable level. Use  $2 \times$  down imaging for the first image,  $4 \times$  down imaging for the second image, and  $8 \times$  down imaging for each subsequent image. Generally, the ability of the transform sparse basis to transform the signal sparsely is expressed by the decay rate of the transform coefficient:

$$v = \left| \frac{r}{d} \right| - \beta \times (|\bar{\mu}| \times \varpi^3) \quad (5)$$

In Eq. (5),  $r$  refers to the orthogonal transformation set,  $d$  refers to the transformation coefficients, and  $\beta$  refers to the coefficient index representation after the coefficients are arranged in power exponential descending order. According to the calculation results of formula (5), the most critical step for unequal interval variable density imaging is the selection and definition of sampling density. In this paper, we choose to conduct under sampling in the direction of  $x$  axis, that is, the size of sampling interval in the direction of  $x$  axis affects the sampling density. Compared with the film as a whole, the high sampling rate of the first two images will not significantly increase the film sampling rate, so it will not have a significant impact on the average sampling time. Nuclear magnetic resonance imaging of medical devices uses the resonance effect of atomic nuclei to image the human body by collecting the electromagnetic signals released after nuclear resonance. Theoretical analysis shows that the total variation regularization constraint can not only reduce the noise in the reconstructed image, but also smooth the edge of the image. However, due to the piecewise smoothness of the image, the piecewise constraint sometimes directly leads to the excessive blur of the fine texture structure of the image. The number of hydrogen atoms in the human body is the largest and the most widely distributed. When imaging the human body with nuclear magnetic resonance medical devices, the resonance effect of hydrogen atoms is generally used to detect its resonance signal. However, wavelet basis function has the characteristics of good time-domain locality and moment cancellation, and can well represent the mutation characteristics of image signals, such as jumping singularity, and well represent the local smooth part. Due to the different content of hydrogen atoms in different parts and tissues of the human body, the detected signal intensity is also different when imaging different parts with NMR medical devices. Therefore, the resonance effect of hydrogen atoms can be used to image human tissues and distinguish pathological tissues.

## 5 Optimization of Intelligent Imaging Mode Based on Compressed Sensing

Compressed sensing is mainly composed of three parts: signal sparse representation, random signal acquisition, i.e. linear measurement process, and sparse reconstruction. Compared with the traditional data compression method, the most distinctive feature of compressed sensing is that it bypasses the inefficient link of sampling and then compression, and uses the sensing matrix to directly obtain the characteristic information of sparse signals or compressible signals. The premise of using compressed sensing is that the signal is sufficiently sparse. Because the actual measured signal is usually not sufficiently sparse, a suitable transform basis is selected to make the signal more sparse in the transform domain, so as to obtain better reconstruction results. If the original signal with sparse representation is sampled randomly, the original signal can be recovered under the condition of breaking through Nyquist. The compressed sensing algorithm breaks through the limitation of Nyquist Shannon sampling theorem, and can greatly reduce the sampling rate of the signal, and accurately reconstruct the original signal with only a small amount of sampling data [9, 10]. In the theory of compression sensing, the linear measurement process is often represented by a stable set of linear equations. The main process of compression sensing is shown in Fig. 1:

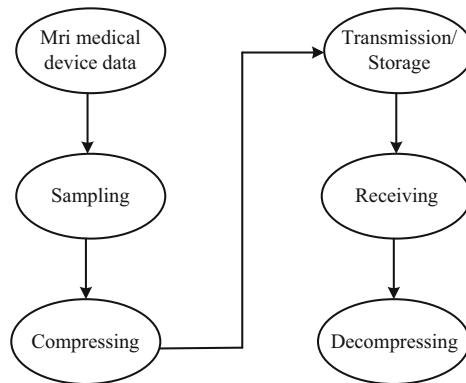


**Fig. 1.** Main process of compression sensing

It can be seen from Fig. 1 that in the imaging process, the signal can be compressed while sampling, reducing the compression cost of the signal. Applying compressed sensing technology to the measurement process of atomic force microscope can reduce the sampling rate of atomic force microscope and shorten the originally long imaging time. The process of intelligent imaging is to use reconstruction algorithm to reconstruct the original signal according to the collected data and measurement matrix. Before explaining the structure of the discriminator, first of all, it briefly introduces the content of the loss function related to the training of the discriminator [11]. In the previous research, the loss function used by the traditional generation countermeasure network in training the generator has two types, one is saturated and the other is unsaturated.

Conduct continuous magnetic resonance imaging operations for many times in a certain time period to capture the operation of human organs and tissues in that time period. Unlike static magnetic resonance imaging, intelligent imaging requires faster imaging speed. And due to the reduction of sampling rate, the interaction force between the probe tip of the atomic force microscope and the sample surface is reduced, so as to reduce the wear of the probe and the damage of the sample surface, and further improve the imaging accuracy of the atomic force microscope. Because the time-varying of human organs and tissues, such as the heart, is moving all the time, and the corresponding space will also change with it [12, 13]. To capture the spatial data at the current time point, we need a very fast data acquisition speed to ensure that the data acquisition is completed before the heart shape changes, otherwise it will inevitably cause data distortion. Under some conditions, when the real data is completely distinguished from the generated data, the saturation loss tends to have a gradient of zero, while the unsaturated loss, although the gradient is not zero, has the problem of instability. This will eventually lead to the discriminator often unable to train to the optimal or the learning rate is too high, otherwise it may make the gradient disappear and the training stop. Therefore, it is necessary to minimize the time of data acquisition without sacrificing spatial resolution.

## 6 Simulation Experiment Analysis

### 6.1 Experimental Preparation

It is composed of NMR spectrometer, RF power amplifier, gradient power amplifier, preamplifier, unilateral NMR equipment, duplexer and computer. CUDA architecture is composed of CPU and GPU. CPU plays the role of host and GPU plays the role of device. Among them, GPU mainly completes threaded parallel processing, while CPU is mainly responsible for serial computing and logical transaction processing. Use coaxial cable to connect the unilateral NMR equipment with the spectrometer. They all have relatively independent memory address space. CPU corresponds to host side memory and GPU corresponds to device side memory. CUDA calls the memory management function in CUDA API to realize the operation of memory and video memory. First, the two-phase coded pulse sequence is written in the tnmr sequence editing software of tecmag NMR spectrometer, and the imaging parameters are set. The NMR signal generated by the sample is directly output to the NMR spectrometer after being amplified by the preamplifier after passing through the duplexer, and then transmitted to the computer, which displays the signal. During the whole experiment, the RF coil has two functions: transmitting and receiving. The operation of memory is basically the same as that of general C programs. The operation of memory mainly includes opening up space, initializing space, releasing space, and completing data transmission at the device end and the host end.

### 6.2 Experimental Result

In order to get intuitive experimental results, the intelligent imaging method of MRI medical devices based on deep learning and the intelligent imaging method of MRI

medical devices based on generation countermeasure network are selected to compare with the intelligent imaging method of MRI medical devices in this paper. Test the peak signal-to-noise ratio of the three MRI medical device intelligent imaging methods under different signal-to-noise ratio conditions. The larger the value, the higher the accuracy. The experimental results are shown in Tables 1, 2, 3 and 4:

**Table 1.** Signal to noise ratio 10 dB peak signal to noise ratio

Number of experiments	Intelligent imaging method of magnetic resonance medical devices based on deep learning	Intelligent imaging method of magnetic resonance medical devices based on generated countermeasure network	The intelligent imaging method of NMR medical devices in this paper
1	21.203	23.655	29.363
2	22.166	22.421	28.345
3	21.245	21.944	31.266
4	23.123	22.106	30.151
5	22.331	21.303	29.009
6	21.228	23.005	31.154
7	22.545	22.146	29.136
8	21.612	20.616	28.483
9	22.144	21.074	27.212
10	21.714	23.099	31.514
11	23.162	24.548	29.217
12	22.495	23.316	28.649
13	21.317	22.157	27.157
14	22.445	21.159	29.166
15	21.147	23.301	30.337

It can be seen from Table 1 that when the signal-to-noise ratio is 10 dB, the peak signal-to-noise ratio of the intelligent imaging method of nuclear magnetic resonance medical devices in this paper and the other two intelligent imaging methods of nuclear magnetic resonance medical devices are 29.0344, 21.992 and 22.390 respectively.

It can be seen from Table 2 that when the signal-to-noise ratio is 30 dB, the average peak signal-to-noise ratio of the NMR medical device intelligent imaging method in this paper and the other two NMR medical device intelligent imaging methods are 45.395, 34.656 and 33.494 respectively.

It can be seen from Table 3 that when the signal-to-noise ratio is 50 dB, the average peak signal-to-noise ratio of the NMR medical device intelligent imaging method in this

**Table 2.** Signal to noise ratio 30 dB peak signal to noise ratio

Number of experiments	Intelligent imaging method of magnetic resonance medical devices based on deep learning	Intelligent imaging method of magnetic resonance medical devices based on generated countermeasure network	The intelligent imaging method of NMR medical devices in this paper
1	32.154	36.474	42.944
2	35.811	32.151	43.847
3	34.326	32.215	45.554
4	32.177	31.933	46.564
5	31.494	34.467	44.518
6	33.547	32.485	43.334
7	36.315	31.120	45.102
8	34.194	34.648	43.174
9	35.477	32.971	46.946
10	36.515	31.479	45.994
11	36.152	34.944	46.741
12	34.483	33.154	48.166
13	35.788	35.747	46.331
14	34.455	33.316	46.559
15	36.949	35.299	45.144

**Table 3.** Signal to noise ratio 50 dB peak signal to noise ratio

Number of experiments	Intelligent imaging method of magnetic resonance medical devices based on deep learning	Intelligent imaging method of magnetic resonance medical devices based on generated countermeasure network	The intelligent imaging method of NMR medical devices in this paper
1	42.313	43.347	48.202
2	43.255	41.152	46.147
3	41.649	42.474	52.105
4	42.636	44.518	49.947
5	41.552	43.166	48.466

*(continued)*

**Table 3.** (continued)

Number of experiments	Intelligent imaging method of magnetic resonance medical devices based on deep learning	Intelligent imaging method of magnetic resonance medical devices based on generated countermeasure network	The intelligent imaging method of NMR medical devices in this paper
6	43.255	41.481	49.747
7	42.144	42.121	51.946
8	41.263	43.333	52.441
9	42.102	42.154	52.646
10	43.447	41.744	51.488
11	44.894	42.849	52.117
12	43.548	44.556	52.599
13	42.474	42.314	53.415
14	41.165	43.415	55.116
15	42.415	41.112	49.212

paper and the other two NMR medical device intelligent imaging methods are 51.040, 42.541 and 42.684 respectively.

**Table 4.** Signal to noise ratio 70 dB peak signal to noise ratio

Number of experiments	Intelligent imaging method of magnetic resonance medical devices based on deep learning	Intelligent imaging method of magnetic resonance medical devices based on generated countermeasure network	The intelligent imaging method of NMR medical devices in this paper
1	52.447	49.994	55.748
2	49.752	48.516	56.851
3	46.188	51.054	58.263
4	48.146	50.477	57.499
5	49.258	52.366	56.205
6	51.481	53.845	57.211
7	49.515	49.211	55.171
8	49.499	48.314	56.447
9	51.515	46.151	57.211

(continued)

**Table 4.** (continued)

Number of experiments	Intelligent imaging method of magnetic resonance medical devices based on deep learning	Intelligent imaging method of magnetic resonance medical devices based on generated countermeasure network	The intelligent imaging method of NMR medical devices in this paper
10	50.162	47.207	58.319
11	48.147	46.499	56.408
12	49.311	48.515	58.523
13	48.487	50.212	56.545
14	51.941	49.324	57.641
15	52.157	48.544	55.109

It can be seen from Table 4 that when the signal-to-noise ratio is 70 dB, the peak signal-to-noise ratio of the intelligent imaging method of nuclear magnetic resonance medical devices in this paper and the other two intelligent imaging methods of nuclear magnetic resonance medical devices are 56.877, 49.867 and 49.349 respectively.

**Table 5.** Signal to noise ratio 90 dB peak signal to noise ratio

Number of experiments	Intelligent imaging method of magnetic resonance medical devices based on deep learning	Intelligent imaging method of magnetic resonance medical devices based on generated countermeasure network	The intelligent imaging method of NMR medical devices in this paper
1	53.991	55.488	62.164
2	52.415	57.415	63.314
3	51.547	56.549	62.331
4	53.316	54.211	61.158
5	54.448	55.099	63.207
6	52.220	56.147	62.849
7	53.147	55.305	63.541
8	54.466	55.488	62.662
9	52.848	56.501	63.315
10	53.502	54.215	64.548
11	54.433	53.490	63.547
12	55.548	54.155	62.644
13	54.699	55.649	63.102
14	53.147	56.007	62.106
15	52.331	54.413	63.113

It can be seen from Table 5 that when the signal-to-noise ratio is 90 dB, the average peak signal-to-noise ratio of the NMR medical device intelligent imaging method in this paper and the other two NMR medical device intelligent imaging methods are 62.907, 53.471 and 55.342 respectively. It can be seen from the experimental results in Tables 1, 2, 3, 4, and 5 that the intelligent imaging method of NMR medical devices in this paper can maintain good performance under different signal-to-noise ratio experimental scenarios.

## 7 Conclusion

- (1) This paper discusses the sparse representation of MRI images in different transform domain spaces, and designs and implements the spatial sparse sampling track with random variable density. At the same time, it studies the peak signal to noise ratio of the intelligent imaging method of MRI medical devices.
- (2) The variance of image pixels is used to adaptively estimate the weighting matrix, which is solved under the framework of compressed sensing. A random variable density sampling method is designed to collect low-frequency regions with high information content.
- (3) The intelligent imaging method of MRI medical devices studied in this paper can maintain good performance in different SNR experimental scenarios.

In the future, it is necessary to continue in-depth research to find an efficient reconstruction algorithm suitable for MRI application scenarios and parallelize it.

**Fund Project.** Project supported by the Scientific Research Foundation of Jimei University, China, ZQ2019034, and Fujian Province Young and Middle-aged Teachers Education Research Project, JAT190303.

## References

1. Wang, M., Wang, Y., Yu, M., et al.: Preliminary application of artificial intelligence-based image optimization in coronary CT angiography. *Chin. J. Radiol.* **54**(5), 460–466 (2020)
2. Phasinam, K., Kassanuk, T.: Machine learning and internet of things (IoT) for real-time image classification in smart agriculture. *ECS Trans.* **107**(1), 3305–3311 (2022)
3. Li, S., Zhang, X., Gao, X., Sun, H.: Research on black-and-white image processing method of smart car camera. *J. Meas. Sci. Inst.* (2), 23–26 (2022)
4. Chierchie, F., Moroni, G.F., Stefanazzi, L., et al.: Smart readout of nondestructive image sensors with single photon-electron sensitivity. *Phys. Rev. Lett.* **127**(24), 1–6 (2021)
5. Li, Y., Chen, Y., Yang, X.: Edge segmentation of brain tumor based on MRI image. *Comput. Simul.* **37**(10), 369–373 (2020)
6. Cai, W., Wang Y.: Advances in construction of human brain atlases from magnetic resonance images. *Chin. J. Magn. Reson.* **37**(2), 241–253 (2020)
7. Li, Q., Zhu, H., Huang, G., et al.: Low-power in-pixel buffer circuit for smart image sensor. *Sens. Rev.* **40**(5), 585–590 (2020)
8. Fan, J., Ma M., Zhao, S.: Research on high reflective imaging technology based on compressed sensing. *J. Electron. Inf. Technol.* **42**(4), 1013–1020 (2020)

9. Xia, K., Yin, H., Jin, Y., et al.: Cross-domain brain CT image smart segmentation via shared hidden space transfer FCM clustering. *ACM Trans. Multimedia Comput. Commun. Appl. (TOMM)* **16**(2), 1–21 (2020)
10. Bao, Y., Cai, M., Zhao, M., et al.: A comparative research on the efficiency and image quality between manual and artificial intelligence post-processing of coronary CT angiography. *J. Pract. Radiol.* **36**(8), 1322–1325 (2020)
11. Wang, W., Zhang, X., Wang, S.-H., Zhang, Y.-D.: Covid-19 diagnosis by WE-SAJ, systems science & control. *Engineering* **10**(1), 325–335 (2022). <https://doi.org/10.1080/21642583.2022.2045645>
12. Huang, C., Wang, W., Zhang, X., Wang, S.-H., Zhang, Y.-D.: Tuberculosis diagnosis using deep transferred EfficientNet. In: *IEEE/ACM Transactions on Computational Biology and Bioinformatics* (2022). <https://doi.org/10.1109/TCBB.2022.3199572>
13. Hida, Y., Makariou, S., Kobayashi, S.: Smart image inspection using defect-removing autoencoder - ScienceDirect. *Procedia CIRP* **104**(1), 559–564 (2021)